Journal of Inorganic and General Chemistry
ZAAC
Zeitschrift für anorganische und allgemeine Chemie
www.zaac.wiley-vch.de
RESEARCH ARTICLE
DOI: 10.1002/zaac.202400025

Cation-Dependent Nuclearity of New Homoleptic Azidocuprates(II), From Discrete Ions to Anionic Strands and Sheets

Alexander Hinz*[a] and Martin Köckerling*[b, c]

Dedicated to Prof. Martin Jansen on the occasion of his 80th birthday.

In chemical reactions of copper(II) acetate dihydrate with imidazolium azide salts in ethanol solution several new homoleptic azidocuprates(II) were obtained. In dependency of the used counter cation various different azidocuprate moieties were crystalized. The doubly charged $DMMDIm^{2+}$ cation facilitates the formation of mononuclear $[Cu(N_3)_4]^{2-}$ complex anions, while the utilisation of the $(PeMIm)^+$ ion enables the isolation of a dinuclear $[Cu_2(N_3)_6]^{2-}$ salt. By using the unsymmetrical imidazolium ions $(BMIm)^+$ or $(EMIm)^+$ salts with the trinuclear $[Cu_3(N_3)_8]^{2-}$ complex anion are obtained. With the $(DML)^+$ cation an azidocuprate(II) crystallizes, which contains both $[Cu(N_3)_4]^{2-}$ and the $[Cu_2(N_3)_6]^{2-}$ anion. The anions in the salt with the $(PeMIm)^+$ cation are interconnected through further Cu–N bonds and form layers with a 2D-honeycomb structure. The trinuclear units in the $(BMIm)^+$ and the $(EMIm)^+$ salts form coordination strands of different structures.

Introduction

Whereas metal azides are notable for their explosive properties with various applications in the field of explosives and propellants,[1] organic azides are very useful reagents in organic reactions, especially in azide-alkyne "click" reactions.[2]

Among the pseudo halide ligands in metal coordination compounds, azides are very intriguing, since multifaceted coordination modes are known.[3] For instance, in tetraazidocuprates(II), the most simple case, μ_1-1-coodination is observed. But also, complexes incorporating μ_2-1,1-, μ_2-1,3-, μ_3-1,1,1-, or μ_3-1,1,3-bridging azide ligands and furthermore, μ_4-1,1,3,3- and μ_6-1,1,1,3,3,3-coordination modes are known.[3–4] The range of coordination modes enables a great variety of structural motifs in multinuclear complex formation.

The solid state structure of copper(II) azide has been elucidated in 1968 and features square planar coordinated Cu atoms with μ_2-1,1 azide bridges between the metal centres.[5] Thus, a layered structure is formed. Between the layers, there are longer Cu–N contacts (2.54(1), 2.709(7)Å), including μ_3-1,1,1 and μ_3-1,1,3 coordination modes.

Binary azidocuprates were first isolated and structurally characterised by means of single crystal X-ray structure elucidations by Dehnicke et al.,[6] namely $(PNP)_2[Cu(N_3)_4]$ and $(Ph_4P)_2[Cu_2(N_3)_6]$ ($(PNP)^+$: bis(triphenylphosphine)iminium), thereby confirming two of the stoichiometric compositions of azidocuprates postulated by M. Straumanis and A. Cirulis in already 1943.[7] Several other investigations targeted copper azide complexes incorporating further neutral ligands. Felthouse et al. obtained an unusual doubly μ_2-1,3-bridged copper azide dimer by employing triamines as ligands, while with a diamine, μ_2-1,1-bridged dimers were formed.[8] Moreover, cryptates and other macrocycles were used as auxiliary ligands by Comarmond et al. and Tandon et al., affording mono-, di-, and tetranuclear complexes.[9] Aromatic N-donor ligands as pyridines, bipyridines or nicotinamides afforded new structural motifs.[10] Magnetic coupling between the metal ions within multinuclear azide bridged coordination compounds was shown to be dependent on interatomic distances as well as on coordination modes and bite angles of the azido ligand. Thus, both ferromagnetic and antiferromagnetic coupling via azides was observed.[9b,11]

In 2005, a template effect of the incorporated cation on the formed oligonuclear anionic unit was observed by Saha et al., who prepared up to trinuclear azidocuprates with different ammonium cations.[12] Furthermore, a hexanuclear structural

[a] Dr. A. Hinz
Karlsruher Institut für Technologie (KIT)
Institut für Anorganische Chemie
Engesserstraße 15, Geb. 30.45
76131 Karlsruhe/Germany
E-mail: Alexander.Hinz@kit.edu
[b] Prof. Dr. M. Köckerling
Institut für Chemie
Anorganische Festkörperchemie
Universität Rostock
Albert-Einstein-Str. 3a
D-18059 Rostock/Germany
E-mail: Martin.Koeckerling@uni-rostock.de
[c] Prof. Dr. M. Köckerling
Universität Rostock, Department Life, Light and Matter, Albert-Einstein-Str. 25
D-18059 Rostock/Germany
E-mail: Martin.Koeckerling@uni-rostock.de

Supporting information for this article is available on the WWW under https://doi.org/10.1002/zaac.202400025

motif of copper azide is known.[13] Wu et al. reported on a discrete heptanuclear $[Cu_7(N_3)_{16}]^{2-}$ azidocuprate anion stabilised by a bulky cation, which was in situ generated by condensation of pyridine-2-carbaldehyde and 2-[(pyridin-2-ylmethylene)-amino]ethanol.[14]

A recent publication reports about tri- and tetranuclear copper(II) azido complexes.[15] Non-covalent interactions of $[Cu(N_3)_4]^{2-}$ ions are studied in ref. [16]. Recent work focused on further heteroleptic copper(II) coordination compounds.[17]

Following our interest in the reactivity of ionic liquids with transition metal salts, we investigated the reaction of several imdiazolium azides and copper acetate. We reinvestigated the PNP/azidocuprate system and obtained the unprecedented, largest so far known azidocuprate anion, $[Cu_{11}(N_3)_{24}]^{2-}$ besides the known tetraazidocuprate(II).[18] In this paper we report about five new homoleptic azidocuprates(II), obtained from chemical reactions of imidazolium based azide salts with copper(II) acetate. Besides the synthesis, their solid-state structures, thermal properties and vibrational spectra are reported of (DMMDIm)$[Cu(N_3)_4]$ (**1**) ((DMMDIm)$^{2+}$ = methylene-1,1′-bis(3-methyl-imidazolium), $(DML)_4[Cu(N_3)_4][Cu_2(N_3)_6]$ (**2**) ((DML)$^+$ = dimethyl-lophinium = 1,3-dimethyl-2,4,5-triphenyl-imidazolium), $(PeMIm)_2[Cu_2(N_3)_6]$ (**3**) ((PeMIm)$^+$ = 1,2,3,4,5-pentamethyl-imidazolium), $(BMIm)_2[Cu_3(N_3)_8]$ (**4**) ((BMIm)$^+$ = 1-butyl-3-methyl-imidazolium), and $(EMIm)_2[Cu_3(N_3)_8]$ (**5**) ((EMIm)$^+$ = 1-ethyl-3-methyl-imidazolium). Scheme 1 shows the structures of the cations.

Results and Discussion

Syntheses

The first step to prepare the new azidocuprates is the synthesis of the imidazolium azide salts AN_3 with the cations A = (DMMDIm)$^{2+}$, (DML)$^+$, (PeMIm)$^+$, (BMIm)$^+$, and (EMIm)$^+$, by metathesis reactions of the imidazolium halides with an excess of sodium azide in acetone. The obtained azide salts are dissolved in ethanol and placed in a small vial, which in turn was placed in an equimolar ethanolic solution of copper(II) acetate. Thus, both starting materials are spatially separated. Both solutions were layered with ethanol, until the ethanol layer established contact for diffusion between both starting materials. Typically, after one week, the diffusion is complete, yielding a green solution and black crystals of the azidocuprates **1**–**5**. Single-crystals, suitable for X-ray structure elucidation were easily isolated by decantation of the solution, washing with cold ethanol and drying in vacuo. The total yields range from 41 % (BMIm) to 91 % (DML) with respect to the azide ions. A green by-product of the reaction aiming for $(BMIm)_2[Cu_3(N_3)_8]$ could be isolated in very small amounts, which could be identified as $(BMIm)[Cu_2(OAc)_5][Cu(OAc)_2(H_2O)]_2 \cdot C_2H_5OH$ which is already known from previous investigations.[19] Therefore it can be speculated that the green colour of the supernatant solutions in the other reactions is also attributed to acetate-rich complexes of the type $A[Cu_2(OAc)_5]$.

An alternative to this synthetic protocol for the preparation of the (BMIm)$^+$ and (EMIm)$^+$ salts $(BMIm)_2[Cu_3(N_3)_8]$ (**4**) and $(EMIm)_2[Cu_3(N_3)_8]$ (**5**) is the combination of sodium azide, copper(II) nitrate and the corresponding imidazolium bromide or iodide in ethanol. This leads to faster reactions and higher yields, but microcrystalline products.

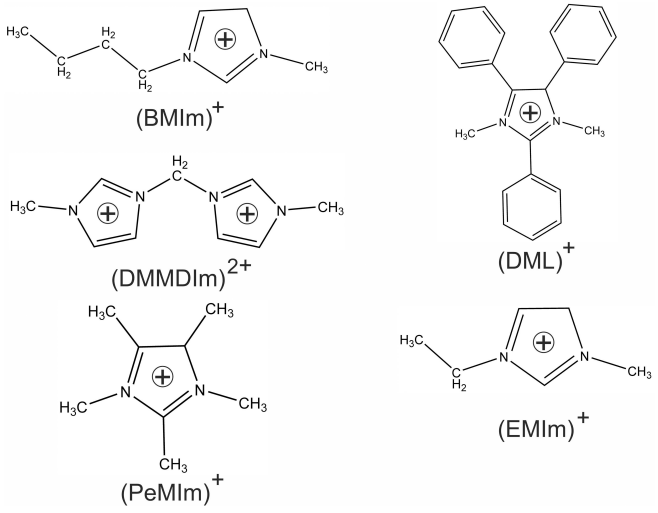

Scheme 1. Structures of the imidazolium cations in the azidocuprates(II).

Thermal Properties

Thermal properties of the new azidocuprates have been investigated by DSC/TA measurements. All of these compounds decompose slowly while releasing nitrogen. No detonation was observed upon heating. The decomposition temperature shows significant dependence on the cation, which is present in the respective salt. The lowest decomposition temperatures were observed for the rather azide rich, small anions (**1** 82 °C, **3** 75 °C). The less azide rich complexes decompose at 114 °C (**5**) and 117 °C (**4**), respectively. The exception to this tendency is $(DML)_4[Cu(N_3)_4][Cu_2(N_3)_6]$ (**2**, 148 °C), but this can be attributed to the much larger cation, which causes a larger interionic distances of the anions and thereby leads to stabilization of the salt. This also applies for the compound with the largest counterions, $(PNP)_2[Cu_{11}(N_3)_{24}] \cdot 2EtOH$, which decomposes at the highest temperature (224 °C).[18]

Vibrational Spectra

Within the imidazolium azide starting materials, the N_3 antisymmetric stretch mode is observed between 1993 and 2000 cm^{-1}. All of the new azidocuprates show the expected strong bands in the IR spectrum well above 2000 cm^{-1}, which are usually combinations of antisymmetric stretching modes.[20] The tetraazidocuprate(II) **1** shows just one band at 2015 cm^{-1}, even though for any case (C_i, C_{2h}, C_{4h} symmetric anion) two antisymmetric stretches are expected. The absence of the second band may be caused by too low resolution. For the

other compounds, more bands are observed. The bands more shifted to higher wave numbers indicate a μ_2-1,1-bridging mode for at least one of the azide ligands, while the less shifted bands can be attributed to end-on coordinated azides, thereby indicating the existence of at least dinuclear anions. Table 1 lists the numerical values of the N_3 stretching modes for the starting materials as well as for the copper complexes. All the spectra are shown in the SI.

Table 1. Wavenumbers (cm^{-1}) of the antisymmetric stretching modes of the imidazolium azide starting materials and the azidocuprates **1**–**5**.

imidazolium azides		azidocuprates	
$(BMIM)N_3$	1995	**1**	2015
$(EMIM)N_3$	1997	**2**	2020, 2027
$(DMMDIm)N_3$	1997	**3**	2018, 2031, 2058
$(DML)N_3$	1993	**4**	2023, 2039, 2048, 2079, 2097
$(PeMIm)N_3$	1995	**5**	2025, 2047, 2093

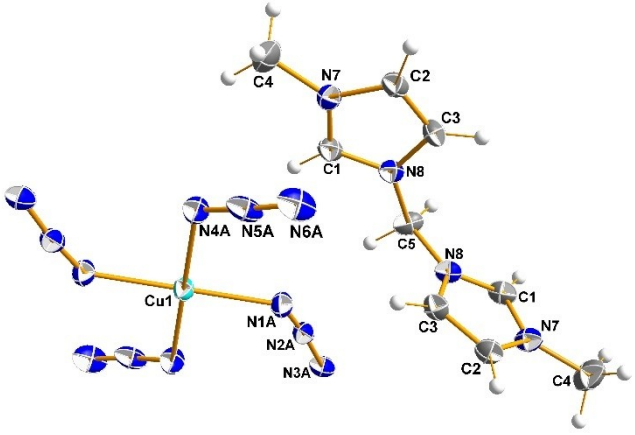

Figure 1. Structure of the ion pair of $(DMMDIm)[Cu(N_3)_4]$ (**1**). Thermal displacement parameters are drawn at the 50% probability level at −150 °C. Only the higher occupied orientation of the disordered complex anion is shown.

Structures

Even though all of the new azidocuprates formally consist of cations and anions, only in case of $(DMMDIm)[Cu(N_3)_4]$ (**1**, Figure 1) and $(DML)_4[Cu(N_3)_4][Cu_2(N_3)_6]$ (**2**) separated, discrete ions are found. In the other three cases the ions are more closely packed, such that distances between ions, shorter than the sum of the van-der-Waals distances, lead to network structures, see below. Selected structural parameters are summarized in Tables 2 and 3, respectively. $(DMMDIm)[Cu(N_3)_4]$ (**1**) crystallises in the monoclinic space group *C*2/*c*. The structure is composed of isolated cations and anions, see Figure 1, in which the tetraazidocuprate anion is disordered. This disorder can be regarded as two orientations of the arrangement of the four azide ions around Cu1, one clockwise (A) and one anti-clockwise (B) in a viewing direction perpendicular to the mean plane through all the atoms of the $Cu(N_3)_4$ units. The refined occupations of the two orientations are 74.4(1)%, and 25.6%, respectively. Figure 2 depicts this disorder. In the following descriptions, only the higher occupied position is referred to. Cu1 is coordinated by four N atoms in a nearly perfect square planar arrangement and is located on a centre of inversion. The N1A–Cu1–N4A and N4A–Cu1–N1A′ angles deviate only slightly from the ideal value of 90°. As expected for metal-coordinated azido ligands, the N_α–N_β bond lengths are longer than the

Table 2. Crystal and structure refinement parameters for **1**–**5**.

	$(DMDIm)[Cu(N_3)_4]$ (**1**)	$(DML)_4[Cu(N_3)_4][Cu_2(N_3)_6]$ (**2**)	$(PeMIm)_2[Cu_2(N_3)_6]$ (**3**)	$(BMIm)_2[Cu_3(N_3)_8]$ (**4**)	$(EMIm)_2[Cu_3(N_3)_8]$ (**5**)
Empirical formula	$C_9H_{14}CuN_{16}$	$C_{92}H_{84}Cu_3N_{38}$	$C_{16}H_{30}Cu_2N_{22}$	$C_{16}H_{30}Cu_3N_{28}$	$C_{12}H_{22}Cu_3N_{28}$
Fw [g·mol^{-1}]	409.90	1912.59	1315.40	805.30	749.19
Crystal system	monoclinic	triclinic	mnoclinic	triclinic	monoclinic
Space group, no.	*C*2/*c*, 15	$P\bar{1}$, 2	$P2_1/c$,14	$P\bar{1}$, 2	$P2_1/n$, 14
a [Å]	22.178(1)	13.527(3)	11.9992(4)	8.3540(5)	5.3342(3)
b [Å]	5.3306(2)	13.629(3)	7.9732(3)	13.1176(8)	24.565(1)
c [Å]	15.8295(7)	13.881(3)	14.4362(5)	14.8968(9)	10.9387(5)
α [°]	90	73.20(3)	90	78.890(3)	90
β [°]	119.169(2)	70.03(3)	91.115(2)	80.861(3)	104.022(3)
γ [°]	90	89.88(3)	90	87.780(3)	90
V [Å^3], *Z*	1634.1(1), 4	2289(1), 1	1380.88(8), 2	1581.5(2), 2	1390.6(1), 2
$2\theta_{max}$ [°], R_{int}	65.3, 0.0386	72.8, 0.0435	55.2, 0.0494	60.9, 0.0648	62.9, 0.1017
T (K)	173(2)	173(2)	173(2)	173(2)	173(2)
GooF on F^2	1.050	1.029	1.030	0.967	0.947
R_1 / wR_2 [$I > 2\sigma(I)$][a]	0.0296 / 0.0773	0.0446 / 0.1220	0.0302 / 0.0751	0.0450 / 0.0753	0.0499 / 0.0890
$\Delta\varrho_{max}$, $\Delta\varrho_{min}$ [e·Å^{-3}]	0.46, −0.30	1.31, −0.60	0.43, −0.27	0.60, −0.61	0.66, −0.66

a) $R1 = \frac{\sum ||F_o| - |F_c||}{\sum |F_o|}$; $wR2 = \sqrt{\frac{\sum w(F_o^2 - F_c^2)^2}{\sum w(F_o^2)^2}}$; b) $w = \frac{1}{\sigma^2(F_o^2)+(AP)^2+BP}$; $P = \frac{F_o^2+2F_c^2}{3}$

Table 3. Ranges of selected atom distances (Å) and angles (°) in the complex anions of **1**–**5** (in case of disordered anions the values of only the most occupied part are given).

	(DMMDIm)[Cu(N$_3$)$_4$], **1**	(DML)$_2$[Cu$_2$(N$_3$)$_6$][Cu(N$_3$)$_4$], **2** [Cu$_2$(N$_3$)$_6$]	[Cu(N$_3$)$_4$]	(PeMIm)$_2$[Cu$_2$(N$_3$)$_6$] **3**	(BMIm)$_2$[Cu$_3$(N$_3$)$_8$] **4**	(EMIm)$_2$[Cu$_3$(N$_3$)$_8$] **5**
Cu–N$_\alpha$ (terminal)	1.986(5)–1.979(4)	1.921(2)–1.949(1)	1.958(1)–1.964(2)	1.955(2)–1.984(2) [a]	1.944(2)–1.975(2)	1.936(3)–1.950(3)
Cu–N$_\alpha$ (bridging)	–	1.990(1)–2.014(2)	–	2.004(2)–2.018(2)	1.963(2)–2.052(2) [b]	2.000(3)–2.052(3) [c]
N$_\alpha$–N$_\beta$	1.191(6)–1.211(7)	1.188	1.195(2)–1.197(2)	1.190(2)–1.203(2)	1.192(3)–1.219(3)	1.190(4)–1.212(4)
N$_\beta$– N$_\gamma$	1.13(2) –1.26(3)	1.134(2)–1.153(2)	1.119(3)–1.13(3)	1.136(3)–1.158(2)	1.136(3)–1.157(3)	1.135(4)–1.153(4)
Cu···Cu	–	3.129(1)	–	3.1507(4)	3.0962(5), 3.1154(5)	3.1100(4)
N$_\alpha$–N$_\beta$–N$_\gamma$	173(1)–174(1)	175.4(2)–177.7(2)	175.1(3)–175.6(2)	176.7(2)–197.2(2)	175.7(3)–178.6(3)	174.9(4)–178.7(4)
N$_\beta$–N$_\alpha$–Cu	120.6(4)–121.0(4)	12.3(1)–132.9(1)	122.1(2)–125(1)	120.5(1)–132.2(1)	118.0(2)–133.2(2)	121.8(3)–131.8(2)
N$_\alpha$–Cu–N$_\alpha$ (cis) (range, average)	89.5(2)–90.5(2)	77.21(6)–101.08(7), 90.47	89.74(8)–90.26(8) 90.00	76.84(7)–97.26(7) 89.49	76.90(9)–101.67(9) 89.93	77.2(1)–100.9(1) 90.02
Cu–N$_\alpha$–Cu	–	102.79(6)	–	103.16(7)	100.5(1)–103.7(1) [b]	100.2(1)–103.2(1) [c]

[a]) Intermolecular Cu–N$_\alpha$ distance: 2.355(2) Å. [b]) Intermolecular Cu–N$_\alpha$ distance and Cu–Nα–Cu angle: 2.408(2) Å, 106.3(1)°, 2.487(2) Å, 100.9(1)°. [c]) Intermolecular Cu–N$_\alpha$ distance and Cu–Nα–Cu angle: 2.675(3) Å, 92.2(1)°, 2.717(3) Å, 89.9(1)°

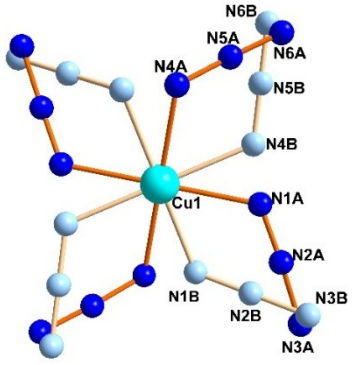

Figure 2. View of the two different orientations of the azido ligands around the Cu(II) atom. In crystals of (DMMDIm)[Cu(N$_3$)$_4$] (**1**).

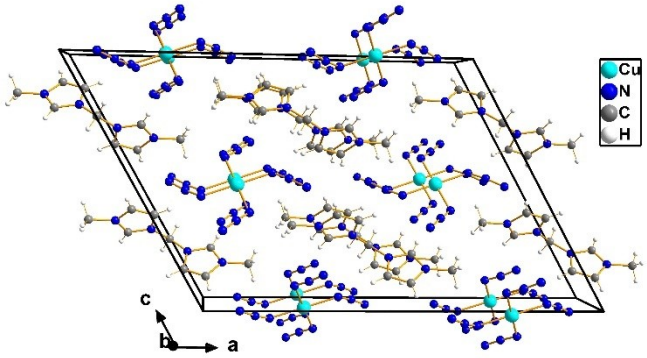

Figure 3. Packing of the ions in (DMMDIm)[Cu(N$_3$)$_4$] (**1**) in a view approx. along the b direction. Minor occupied parts of the disordered azide anions are not shown.

corresponding N$_\beta$–N$_\gamma$. Due to the influence of the disorder the difference is very small.

Figure 3 shows the packing of the ions in the unit cell. The distance between the Cu atoms of two neighbouring complex anions corresponds to the length of the *b* axis and is therefore clearly out of the range of any bonding interactions.

In (DML)$_4$[Cu(N$_3$)$_4$][Cu$_2$(N$_3$)$_6$] (**2**) half of the formula unit comprises the asymmetric unit. The compound consists of [Cu(N$_3$)$_4$]$^{2-}$ ions, [Cu$_2$(N$_3$)$_6$]$^{2-}$ ions, and (DML)$^+$ cations. It can be described as double salt (DML)$_2$[Cu(N$_3$)$_4$]·(DML)$_2$[Cu$_2$(N$_3$)$_6$]. In the crystals both azidocuprate anions reside on inversion centres. Similar as in **1** the azide units of the [Cu(N$_3$)$_4$]$^{2-}$ ion are arranged around the Cu atom in two different orientations, treated in the refinements by a split model. The orientation A is occupied by 84.6(2) % and B by 15.4 %, respectively. Further disordered structural motifs are observed within the cations. In each cation of the asymmetric unit one of the phenyl rings adopts different orientations, what has been treated again with split models in the refinements. The structure of the ions is shown in Figure 4. All Cu atoms in both anions are coordinated in a square planar geometry, i. e. all atoms in both anions are arranged within a common plane. The centrosymmetric, dinuclear [Cu$_2$(μ$_2$-1,1-N$_3$)$_2$(N$_3$)$_4$]$^{2-}$ anion in **2** has one of the terminal azide ions per Cu atom arranged almost parallel to the bridging azide. This ligand arrangement is also present in **3** (see below) and has been found before in (Bu$_4$N)$_2$[Cu$_2$(N$_3$)$_6$] (Bu = n-butyl).[12] A different arrangement with all terminal azide ions being arranged perpendicular to the bridging azide ions is found in (Ph$_4$P)$_2$[Cu$_2$(N$_3$)$_6$].[6a] Thereby, the symmetry of the complex ions are different, C$_{2h}$ in **2** and D$_{2h}$ in the last mentioned unit.

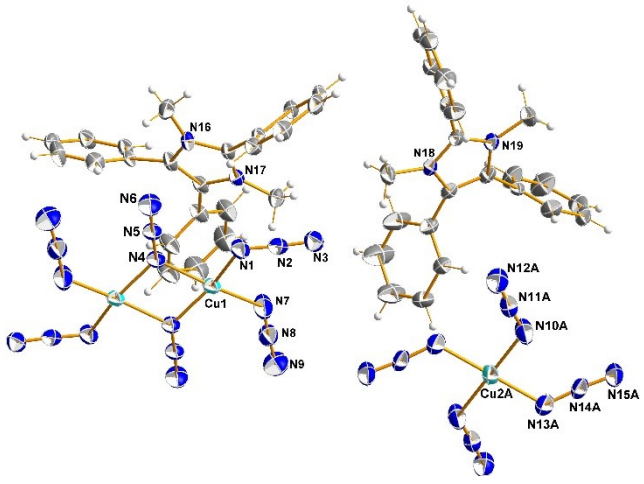

Figure 4. Structure of the ions of $(DML)_4[Cu(N_3)_4][Cu_2(N_3)_6]$ (**2**). Thermal displacement parameters are drawn at the 50% probability level at −150 °C. Only the higher occupied orientations of the disordered structural parts are shown.

The azidocuprates with the cations $(PeMIm)^+$ (**3**), $(BMIm)^+$ (**4**), and $(EMIm)^+$ (**5**) differ from **1** and **2**, because they do not consist of discrete ions, but coordination polymers.

$(PeMIm)_2[Cu_2(N_3)_6]$ (**3**) crystallises in the monoclinic space group $P2_1/n$. The cation has local (not crystallographic) five-fold symmetry and the N atoms are statistically distributed over all five ring positions. The molecular structure of one ion pair is shown in Figure 5. The dinuclear anions are arranged such that each N3 atom is located above one of the copper atoms of a neighbouring anion. Thereby each Cu atom is coordinated tetragonal pyramidal with the intermolecular Cu–N3′ distance being slightly longer than the intramolecular Cu–N distances (see below). This leads to an anionic coordination polymer with a honeycomb structure, shown in Figure 6A. Since the anions are basically flat the polymer extends in two dimensions, i.e. within the crystallographic b-c plane. The $(PeMIm)^+$ cations are located above and below the cavities of the honeycombs (Figure 6B), also in layers. Along the crystallographic *a* axis, alternating layers of cations and anionic are found, see Figure 7.

$(BMIm)_2[Cu_3(N_3)_8]$ (**4**, Figure 8) crystallises in the triclinic space group $P\bar{1}$. Within the azidocuprate anion four terminal and four μ_2-1,1-bridging azido ligands exist. The three Cu atoms are arranged in a row such that the anion can be regarded as unit of two mononuclear tetraacidocuprate units, connected by a further Cu(II) ion. As in all complex anions, described in this

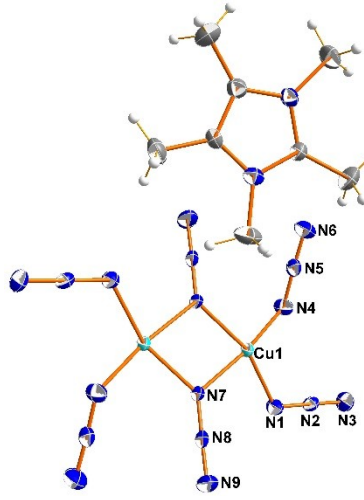

Figure 5. Structure of one ion pair of $(PeMIm)_2[Cu_2(N_3)_6]$ (**3**). Thermal displacement parameters are drawn at the 50% probability level at −150 °C. Of the five orientations of the PeMIm cation only one is shown.

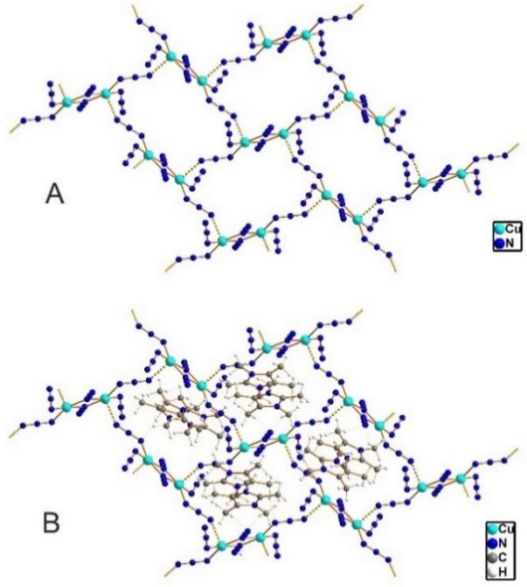

Figure 6. The 2D-layered honeycomb structure of the anions in **3** (A) and the location of the cations above and below the honeycomb cavities (B).

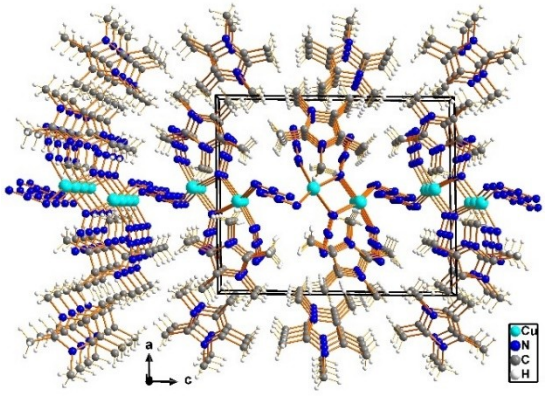

Figure 7. Stacking of the polymeric anionic layers and layers of cations along the crystallographic *a* direction in crystals of $(PeMIm)_2[Cu_2(N_3)_6]$.

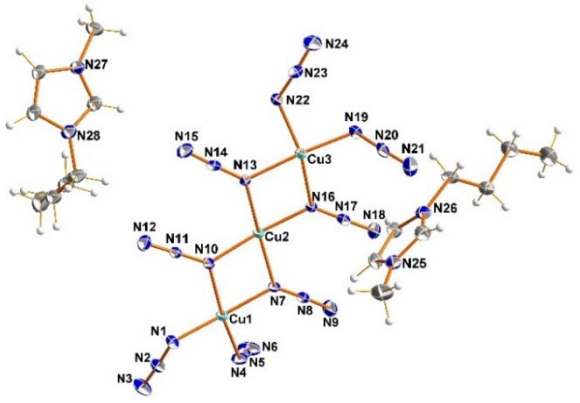

Figure 8. Structure of one ion pair of $(BMIm)_2[Cu_3(N_3)_8]$ (**4**). Thermal displacement parameters are drawn at the 50% probability level at −150 °C.

paper, the copper atoms have a square-planar coordination environment, $Cu(N_\alpha)_4$. Furthermore, all the Cu atoms, the N atoms of the bridging ligands, and the N_α atoms of the terminal ligands are arranged in a common plane. The terminal ligands are bend out of this plane. The dihedral angles between the mean plane through these atoms and the plane through the $Cu–N_\alpha–N_\beta$ atoms are 31.3° for Cu3–N22–N24, 39.4° for Cu1–N1–N2, 56.5° for Cu3–N19–N20, and 73.6° for Cu1–N4–N5. The trinuclear units are arranged in a slipped stack and are connected by interlayer coordination of Cu2 and Cu3′ as shown in Figure 9 (top), extending along the crystallographic a direction. The planar units are piled up and shifted with respect to both neighbouring units, such that two intermolecular contacts Cu2–N22′ (symmetry code 1-x, 1-y, 1-z) and Cu3–N1″ (-x, 1-y, 1-z) exist with distances around ~2.4 Å, shown as red lines in Figure 9 (top). This arrangement differs completely from that of the azidocuprate described in ref. [12] with a trinuclear anion of the same composition. Here, all the azido ligands are bend out of the $Cu_3(N_\alpha)_8$ plane. The trinuclear units are not piled up but interconnected at both ends through the terminal azido ligands such that a coordination strand exists, see Figure 9 (bottom). Thus, the structure of the anion depends strongly on the type of cation, present; $(BMIm)^+$ in the title compound and $(Pr_4N)^+$ in the compound from ref. [12].

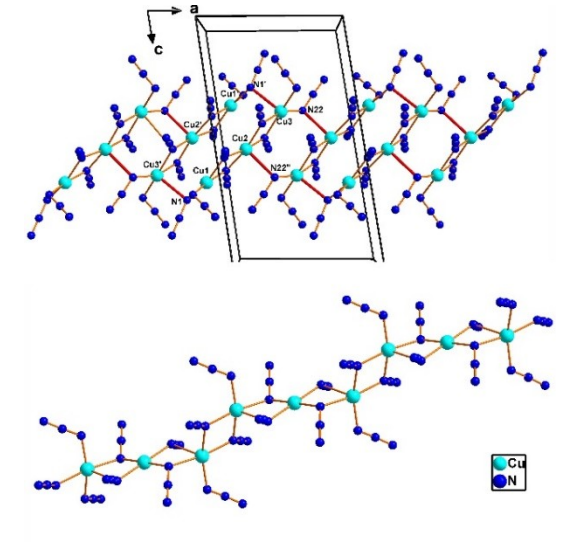

Figure 9. Top: Coordination strand formed by stacking of $[Cu_3(N_3)_8]^{2-}$ units in *(BMIm)*$_2[Cu_3(N_3)_8]$; Bottom: Structure of the strand of the same anion in *(Pr$_4$N)*$_2[Cu_3(N_3)_8]$.[12]

The azidocuprate(II) **5**, $(EMIm)_2[Cu_3(N_3)_8]$, crystallises in the monoclinic system with space group $P2_1/n$. The $[Cu_3(N_3)_8]^{2-}$ moiety has inversion symmetry and is basically planar, see Figure 10. Only the (N10, N11, N12)-azido ligand is bent out of the mean plane by 28°. In the crystal the azidocuprate moieties are stacked on top of each other in a similar way as in **4**, see Figure 11. The resulting coordination strands extend along the crystallographic *a* direction, similar as in **4**. The difference to **4** is that the shift of each anion relative to the neighbouring ones is different. Here 8 contacts, 4 to each side exist with an average intermolecular distance of 2.696 Å, whereas in **4** each anion has only 4 contacts (2 to each side) at a distance of 2.449 Å.

The compounds of this study show that the used cation has a major influence on the nuclearity and structure of the azidocuprate anion, which forms during the synthesis. This is in

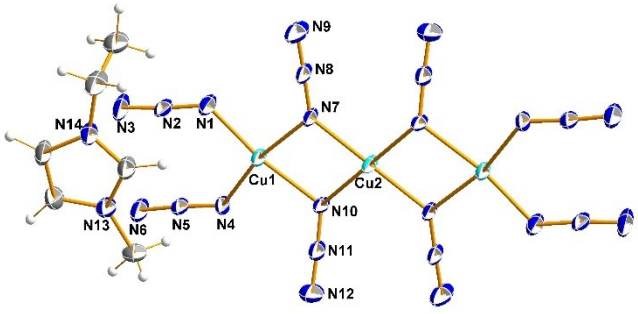

Figure 10. Structure of one ion pair of $(EMIm)_2[Cu_3(N_3)_8]$ (**5**). Thermal displacement parameters are drawn at the 50% probability level at −150 °C.

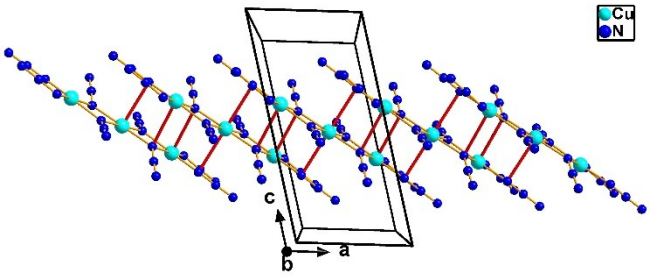

Figure 11. Anionic coordination strand of interconnected $[Cu_3(N_3)_8]^{2-}$ units in crystals of $(EMIm)_2[Cu_3(N_3)_8]$ (**4**). The intermolecular Cu–N bonds around 2.4 Å atom distance are drawn as red lines.

line with the assumption, published before in ref. [12], that the size (nuclearity) of the azidocuprate ion depends strongly on the size (structure) of the cation.

Conclusions

The reactions of cupric acetate with azide salts of organic cations renders a variety of different azidocuprates accessible. Subtle influences of cation, solvent and stoichiometry can lead to a remarkable variety of structural motifs of the resulting azidocuprates(II). Discrete mono- or dinuclear anions could be obtained, but also salts in which the anions form coordination polymers were formed. Thus, studying the cation dependency systematically is required for comprehensive understanding of azidocuprate formation.

Experimental Section

Safety Notes! Azides, especially metallo azides are potentially explosive. They must always be handled with sufficient precaution and should be prepared in small amounts only.

Vibrational spectroscopy: Infrared spectra in the range from 4000 - 500 cm^{-1} were recorded with a Nicolet 380 FTIR spectrometer equipped with a Smart Orbit ATR device.

Decomposition Temperatures: Decomposition temperatures were determined with the aid of a Boetius hot plate equipped with a microscope.

Elemental Analysis: The elemental analyses were accomplished by means of an Analysator Flash EA 1112 from Thermo Quest.

X-ray Crystallography: Data for the X-ray structure determinations were collected on a Bruker-Nonius APEX–X8 or Bruker APEX2 diffractometer equipped with a CCD detector. Graphite monochromated MoK_α radiation ($\lambda = 0.71073$ Å) was used. Single crystals were selected in perfluorinated polyether (Fomblin YR-1800, Alfa Aesar), fixed at the top of a glass fiber and mounted on the goniometer. First unit cell dimensions were determined from the reflections of 36 frames measured in 3 different crystal directions. Data collection was done using the Bruker-Nonius measuring and data reduction software, which includes corrections for absorption, background, Lorenz and polarization effects.[21] The structures were solved by direct methods. The structural models were completed using difference Fourier maps and refined by full-matrix least-squares methods on F^2. All atoms except hydrogen were refined using anisotropic thermal parameters. Hydrogen atoms were fixed on idealized positions and refined with isotropic thermal parameters based on the bonded atom. All calculations were performed using the SHELX version 2014 programs and ShelXle.[22] Further details of the crystal structure investigations are supplied in CIF format. This material is available free of charge via the CCDC data centre, CSD-901885 for **1**, CSD-901887 for **2**, CSD-901886 for **3**, CSD-901875 for **4**, and CSD-901884 for **5**, http://www.ccdc.cam.ac.uk, or from the Cambridge Crystallographic Data Centre, 12 Union Road, Cambridge CB21EZ, UK, Fax: (+44) 1223–336-033, or E-mail: deposit@ccdc.cam.ac.uk

Synthesis

$(DMMDIm)Cl_2$,[23] (PeMIm)I, (DML)I,[24] (EMIm)Cl and (BMIm)Cl[25] are accessible by known syntheses. (PeMIm)Cl und (DML)Cl were prepared from the iodide by metathesis with AgCl. General procedure for the azide salts: The imidazolium chloride is dissolved or suspended in acetone, treated with an excess of NaN_3 and stirred at room temperature for 8 hours. The suspension is filtered off and the filtrate is dried in vacuo.

$(DMMDIm)Cl_2$ (94 mg, 0.38 mmol) and NaN_3 (60 mg, 0.92 mmol) afford 85 mg (0.32 mmol, 85 %) of $(DMMDIm)(N_3)_2$ as pale yellowish solid, mp. 105 °C. EA for $C_9H_{14}N_{10}$, found % (calc. %): C 40.96 (41.21), H 5.60 (5.38), N 52.29 (53.40). IR (ATR, cm^{-1}): 3390w, 3310w, 3228w, 3078w, 3046 m, 3012w, 2992w, 2878w, 2131 m, 1997vs, 1668w, 1581 m, 1557 m, 1543w, 1466w, 1450w, 1403w, 1391w, 1343 m, 1323w, 1309w, 1279w, 1243w, 1211w, 1163 s, 1109 m, 1061w, 1048w, 1022w, 961w, 890w, 882w, 842w, 803w, 763 m, 719w, 665w, 653w, 638 m, 630w, 615w, 601w. NMR ([D_6]-DMSO). ^{1}H: 9.59 (s, 2H, N–CH–N), 7.97 (d, 4H, N–CH-CH–N), 6.78 (s, 2H, N–CH_2-N), 3.91 (s, 6H, N–CH_3). ^{13}C: 138.27, (N–C-N), 124.37, 121.79 (N–C–C–N), 57.98 (N–CH_2-N), 36.18 (N–CH_3).

Conversion of 600 mg (1.32 mmol) (DML)I with 215 mg (1.5 mmol) AgCl affords 402 mg (1.11 mmol, 84 %) of colourless (DML)Cl. Metathesis of NaN_3 (42 mg, 0.65 mmol) with (DML)Cl (193 mg, 0.53 mmol) results in (108 mg, 0.29 mmol, 55 %) a pale yellowish solid, mp. 201 °C. EA for $C_{23}H_{21}N_5$, found % (calc. %): C 74.69 (75.18), H 5.82 (5.76), N 18.39 (19.06). IR (ATR, cm^{-1}): 3283w, 3212w, 3054w, 3024w, 2998w, 2954w, 1993vs, 1706w, 1633w, 1594w, 1514 m, 1487 m, 1462w, 1443n, 1415w, 1395w, 1357 m, 1333w, 1324w, 1278w, 1222w, 1184w, 1157w, 1077w, 1057w, 1024 m, 997w, 860w, 829w, 771 m, 755 s, 695vs, 633w, 616w. NMR in CD_3OD. ^{1}H: 6.28 (m, 5H, N–CPh–N), 5.94 (m, 10H, N–CPh-CPh–N), 2.08 (s, 6H, N–CH_3). ^{13}C: 146.42 (N–C-N), 134.11, 133.84, 132.17, 131.90, 131.58, 131.16, 130.36, 127.17, 123.62, (N–C–C–N), 35.17, (N–CH_3).

The reaction of (PeMIm)Cl (72 mg, 0.41 mmol) with NaN_3 (32 mg, 0.49 mmol) affords a pale orange solid (65 mg, 0.36 mmol, 88 %), mp. 45 °C. EA for $C_8H_{15}N_5$, found % (calc. %): C 52.04 (53.02), H 9.02 (8.34), N 37.13 (38.64). IR (ATR, cm^{-1}): 3303w, 3225w, 3014w, 2992w, 2956w, 2930w, 2873w, 1995vs, 1731w, 1651 m, 1547 m, 1537 m, 1447 m, 1405w, 1372w, 1353w, 1234 m, 1126w, 1077w, 1044w, 1020w, 990w, 832 m, 653w, 629w, 580w, 562w. NMR in [D_6]-DMSO. ^{1}H: 3.63 (s, 6H, N–CH_3), 2.59 (s, 3H, N–C-(N)-CH_3), 2.22 (s, 6H, C–C–CH_3). ^{13}C: 142.70 (N–C-N), 125.03 (N–C–C–N), 31.57 (N–CH_3), 9.60 (N–C-(N)-CH_3), 8.00 (C–C–CH_3).

Metathesis of NaN_3 (413 mg, 6.3 mmol) with (BMIm)Cl (1.001 g, 5.7 mmol) affords 992 mg (5.5 mmol, 96 %) of an orange liquid, mp. −86 °C (glas transition). EA for $C_8H_{15}N_5$, found % (calc. %): C 53.51 (53.02), H 9.14 (8.34), N 38.23 (38.64). IR (ATR, cm^{-1}): 3302w, 3141w, 3068w, 2958 m, 2934w, 2872w, 1995vs, 1707 m, 1566 m, 1462 m, 1427w, 1381w, 1363w, 1336w, 1223w, 1166 s, 1115w, 1092w, 1020w, 929w, 847w, 753w, 697w, 652w, 620 m, 530w. NMR in [D_6]-DMSO. ^{1}H: 9.23 (s, 1H, N–CH–N), 7.77 (d, 2H, N–CH-CH–N), 4.18 (t, 2H, N–CH_2-CH_2), 3.86 (s, 3H, N–CH_3), 1.76 (m, 2H, N–CH_2-CH_2), 1.25 (m, 2H, CH_2-CH_3), 0.88 (t, 3H, CH_2-CH_3). ^{13}C: 136.66 (N–C-N), 123.61, 122.30 (N–C–C–N), 48.50 (N–CH_3), 35.67 (N–CH_2), 31.37 (N–CH_2-CH_3), 18.77 (CH_2-CH_3), 13.24 (CH_2-CH_3).

Metathesis of NaN_3 (124 mg, 1.91 mmol) with (EMIm)Cl (254 mg, 1.73 mmol) affords 214 mg (1.40 mmol, 81 %) of a red liquid. EA for $C_6H_{11}N_5$, found % (calc. %): C 46.12 (47.04), H 8.10 (7.24), N 44.87 (45.72). IR (ATR, cm^{-1}): 3307w, 3145w, 3079w, 2982w, 1997vs, 1644w, 1567 m, 1450w, 1427w, 1386w, 1333w, 1299w, 1252w, 1166 s, 1088w, 1022w, 959w, 841w, 755w, 701w, 647w, 619 m, 596w. NMR in [D_6]-DMSO. ^{1}H: 9.19 (s, 1H, N–CH–N), 7.76 (d, 2H, N–CH-CH–N), 4.19 (q, 2H, N–CH_2-CH_3), 3.85 (s, 3H, N–CH_3), 1.40 (t, 3H, CH_2-CH_3). ^{13}C: 136.44 (N–C-N), 123.63, 122.05 (N–C–C–N), 44.22 (N–CH_3), 35.67 (N–CH_2), 15.14 (CH_2–CH_3).

The obtained azide salts are dissolved in ethanol (0.2 mmol: BMIm 35 mg, EMIm 31 mg, 1/2 DMMDIm 27 mg, PeMIm 35 mg, DML 73 mg). The solution is placed in a small vial. This vial is placed in a solution of 40 mg (0.1 mmol, dimeric) copper acetate dihydrate in ethanol. Both components are layered with ethanol until both solutions are connected and left undisturbed for one week. Within this time, black crystals are formed. The green solution is decanted, the crystals are washed with small amounts of cold ethanol and dried in vacuo. Yields are referred to the amount of azides.

Alternatively, the BMIm and EMIm compounds can be obtained in higher yields by combining $Cu(NO_3)\cdot 3\,H_2O$ (0.2 mmol), (BMIm)Br/(EMIm)Br (0.2 mmol) and NaN_3 (1.2 mmol) in ethanol. Upon combining the components, immediately a dark suspension is formed. The mixture is stirred for one hour at room temperature, filtered off, washed with a small amount of cold ethanol and dried in vacuo. Yields: 62% (BMIm), 89% (EMIm).

*(DMMDIm)[Cu(N$_3$)$_4$] (**1**).* (68% yield). T_{dec} 82 °C. EA $CuC_9H_{14}N_{16}$, found % (calc %): C 25.89 (26.37), H 3.38 (3.44), N 52.39 (54.68). IR (ATR, cm^{-1}): 3130w, 3099 m, 3062 m, 2015vs, 1682w, 1615w, 1581 m, 1548 m, 1455w, 1417w, 1392w, 1334 m, 1279 m, 1162 m, 1104w, 1087w, 1042w, 1017w, 856w, 769w, 743 m, 675w, 619 m, 607w.

*(DML)$_4$[Cu(N$_3$)$_4$][Cu$_2$(N$_3$)$_6$] (**2**).* (91% yield). T_{dec} 148 °C. EA $Cu_3C_{92}H_{84}N_{37.72}Cl_{0.09}$, found % (calc %): C 60.75 (57.79), H 4.85 (4.43), N 26.64 (27.63). IR (ATR, cm^{-1}): 3338w, 3305w, 3055w, 2953w, 2062w, 2027vs, 2020vs, 1510 m, 1506 m, 1486 m, 1455w, 1442 m, 1413w, 1393w, 1335w, 1284 m, 1179w, 1156w, 1074w, 1055w, 1024 m, 995w, 932w, 857 m, 786w, 773 m, 757 s, 717w, 699 s, 656w, 609w.

*(PeMIm)$_2$[Cu$_2$(N$_3$)$_6$] (**3**).* (66% yield). T_{dec} 75 °C. EA $Cu_2C_{16}H_{30}N_{22}$, found % (calc %): C 30.09 (29.22), H 4.98 (4.60), N 46.41 (46,86). IR (ATR, cm^{-1}): 2992w, 2956w, 2924w, 2854w, 2058vs, 2031vs, 2018vs, 1650 m 1602w, 1587w, 1539 m, 1435 m, 1388w, 1368w, 1338w, 1300 m, 1289 m, 1236w, 1140w, 1069w, 1037w, 975w, 829 m, 689w, 651 m, 605w, 592w, 581w, 561w.

*(BMIm)$_2$[Cu$_3$(N$_3$)$_8$] (**4**).* (42% yield). T_{dec} 117 °C. EA $Cu_3C_{16}H_{30}N_{28}$, found % (calc %): C 23.56 (23.87), H 3.86 (3.76), N 48.25 (48,70). IR (ATR, cm^{-1}): 3367w, 3324w, 3148 m, 3106 m, 3084w, 2961 m, 2933w, 2872w, 2097 s, 2076 s, 2048vs, 2039sh, 2023vs, 1599 m, 1563 s, 1418 s, 1333 m, 1278 m, 1260s, 1163 m, 1085w, 1019 s, 947w 865w, 835w, 793 m, 764w, 686 m, 653w, 621 m, 579w.

*(EMIm)$_2$[Cu$_3$(N$_3$)$_8$] (**5**).* (51% yield). T_{dec} 114 °C. EA $Cu_3C_{12}H_{22}N_{28}$, found % (calc %): C 18.65 (19.24), H 3.19 (2.96), N 51.74 (52.35). IR (ATR, cm^{-1}): 3163w, 3134w, 3108w, 3081 m, 2986w, 2966w, 2944w, 2093 s, 2047vs, 2025sh, 1610w, 1559 m, 1461w, 1449w, 1427w, 1390w, 1339 m, 1288 m, 1251w, 1161 m, 1114w, 1095w, 1067w, 1032w, 961w, 864 m, 807w, 755n, 702w, 679w, 649 m, 620 m, 592w, 581w.

Author Contributions

All the authors have accepted responsibility for the entire content of this submitted manuscript and approved submission.

Acknowledgements

The authors thank the DFG for financial support. We are indebted to Dr. Tim Peppel for supplying us with some imidazolium salts. Furthermore, Dr. Alexander Villinger's care of the X-ray equipment is gratefully acknowledged. Open Access funding enabled and organized by Projekt DEAL.

Conflict of interest

The authors declare no conflict of interest regarding this article.

Data Availability Statement

The data that support the findings of this study are available in the supplementary material of this article.

Keywords: Copper · Azides · Ionic Liquids · X-ray diffraction · Thermal properties

[1] a) S. Bräse, C. Gil, K. Knepper, V. Zimmermann, *Angew. Chem. Int. Ed. Engl.* **2005**, *44*, 5188–5240; b) M. H. H. Wurzenberger, M. S. Gruhne, M. Lommel, N. Szimhardt, J. Stierstorfer, *Mater Adv* **2022**, *3*, 579–591.
[2] N. K. Devaraj, M. G. Finn, *Chem. Rev.* **2021**, *121*, 6697–6698.
[3] W. P. Fehlhammer, W. Beck, *Z. Anorg. Allg. Chem.* **2013**, *639*, 1053–1082, and references cited therein.
[4] C. Adhikary, S. Koner, *Coord. Chem. Rev.* **2010**, *254*, 2933–2958.
[5] R. Söderquist, *Acta Crystallogr. Sect. B* **1968**, *24*, 450–455.
[6] a) D. Fenske, K. Steiner, K. Dehnicke, *Z. Anorg. Allg. Chem.* **1987**, *553*, 57–63; b) W. Hiller, K. Hösler, K. Dehnicke, *Z. Anorg. Allg. Chem.* **1989**, *574*, 7–13.
[7] M. Straumanis, A. Cīrulis, *Z. Anorg. Allg. Chem.* **1943**, *251*, 315–331.
[8] a) O. L. Casagrande, S. I. Klein, A. E. Mauro, K. Tomita, *Transition Met. Chem.* **1989**, *14*, 45–47; b) T. R. Felthouse, D. N. Hendrickson, *Inorg. Chem.* **1978**, *17*, 444–456.
[9] a) J. Comarmond, P. Plumere, J. M. Lehn, Y. Agnus, R. Louis, R. Weiss, O. Kahn, I. Morgenstern-Badarau, *J. Am. Chem. Soc.* **1982**, *104*, 6330–6340; b) S. S. Tandon, L. K. Thompson, J. N. Bridson, M. Bubenik, *Inorg. Chem.* **1993**, *32*, 4621–4631.
[10] a) M. A. S. Goher, F. A. Mautner, *Polyhedron* **1995**, *14*, 1751–1757; b) M. A. S. Goher, R.-J. Wang, T. C. W. Mak, *J. Mol. Struct.* **1991**, *243*, 179–182; c) L. Li, D. Liao, Z. Jiang, J.-M. Mouesca, P. Rey, *Inorg. Chem.* **2006**, *45*, 7665–7670.
[11] a) S. Koner, S. Saha, T. Mallah, K.-I. Okamoto, *Inorg. Chem.* **2004**, *43*, 840–842; b) I. von Seggern, F. Tuczek, W. Bensch, *Inorg. Chem.* **1995**, *34*, 5530–5547.
[12] S. Saha, S. Koner, J.-P. Tuchagues, A. K. Boudalis, K.-I. Okamoto, S. Banerjee, D. Mal, *Inorg. Chem.* **2005**, *44*, 6379–6385.
[13] T. Liu, Y.-F. Yang, Z.-M. Wang, S. Gao, *Chem. Asian J.* **2008**, *3*, 950–957.
[14] D.-Y. Wu, W. Huang, L. Liu, Y.-X. Han, G.-H. Wu, *Inorg. Chem. Commun.* **2011**, *14*, 667–671.
[15] Y. Zeng, S.-J. Liu, C.-M. Liu, Y.-R. Xie, Z.-Y. Du, *New J. Chem.* **2017**, *41*, 1212–1218.
[16] P. K. Bhaumik, R. M. Gomila, A. Frontera, S. Benmansour, C. J. Gómez-García, S. Chattopadhyay, *New J. Chem.* **2022**, *46*, 11286–11295.
[17] a) M. Ghosh, P. P. Chakrabarty, A. D. Jana, D. Schollmeyer, H. Sakiyama, M. Mikuriya, R. Debnath, P. Brandão, D. Mal, S. Saha, *Inorg. Chim. Acta* **2022**, *531*, 120713; b) G. T. Papanikolaou, K. N. Pantelis, G. Lazari, L. Cunha-Silva, A. Escuer, T. C. Stamatatos, *Polyhedron* **2021**, *206*, 115315.

[18] A. Hinz, M. Köckerling, *ChemistrySelect* **2017**, *2*, 9654–9657.
[19] A. Hinz, M. Köckerling, *Z. Anorg. Allg. Chem.* **2015**, *641*, 1347–1351.
[20] E. Lieber, C. N. R. Rao, A. E. Thomas, E. Oftedahl, R. Minnis, C. V. N. Nambury, *Spectrochim. Acta* **1963**, *19*, 1135–1144.
[21] Bruker, Nonis, *Bruker AXS Inc.* **2008**, *Madison, Wisconsin, USA*.
[22] a) C. B. Hübschle, G. M. Sheldrick, B. Dittrich, *J. Appl. Crystallogr.* **2011**, *44*, 1281–1284; b) G. M. Sheldrick, *Acta Crystallogr.* **1990**, *A46*, 467–473; c) G. M. Sheldrick, *Acta Crystallogr.* **2008**, *A64*, 112–122; d) G. M. Sheldrick, Sheldrick, G. M., University of Göttingen: Göttingen (Germany), **2014**; e) G. M. Sheldrick, *Acta Crystallogr.* **2015**, *A71*, 3–8; f) G. M. Sheldrick, *Acta Crystallogr.* **2015**, *C71*, 3–8.
[23] C. Cao, Y. Zhuang, J. Zhao, H. Liu, P. Geng, G. Pang, Y. Shi, *Synth. Commun.* **2012**, *42*, 380–387.
[24] T. Peppel, P. Thiele, M. Köckerling, *Russ. J. Coord. Chem.* **2012**, *38*, 207–218.
[25] J. G. Huddleston, A. E. Visser, W. M. Reichert, H. D. Willauer, G. A. Broker, R. D. Rogers, *Green Chem.* **2001**, *3*, 156–164.

Manuscript received: February 28, 2024
Revised manuscript received: April 21, 2024
Accepted manuscript online: April 23, 2024